



## Rapid Spectroscopy-based Fingerprinting Combined with Data Fusion Chemometrics of *Amaranthus tricolor* L. for Growing Environment Discrimination

Ayu Muthia<sup>1</sup>, Daimon Syukri<sup>2</sup>, Mai Efdi<sup>1</sup> and Adlis Santoni<sup>1\*</sup><sup>1</sup>Department of Chemistry, Faculty of Mathematics and Natural Sciences, Universitas Andalas, Padang 25163, Indonesia<sup>2</sup>Department of Food and Agricultural Product Technology, Faculty of Agricultural Technology, Universitas Andalas, Padang 25163, Indonesia

## ARTICLE INFO

## ABSTRACT

## Article history:

Received 15 September 2025

Revised 11 October 2025

Accepted 16 October 2025

Published online 01 November 2025

**Copyright:** © 2025 Muthia *et al.* This is an open-access article distributed under the terms of the [Creative Commons Attribution License](#), which permits unrestricted use, distribution, and reproduction in any medium, provided the original author and source are credited.

*Amaranthus tricolor* L. is a nutrient-rich plant with significant health-promoting properties, making it a valuable candidate for functional foods and therapeutic applications. This study investigated the effect of the cultivation environment on the metabolite composition of *A. tricolor* L. by comparing soil- and hydroponically grown samples. Spectral analysis using ultraviolet-visible (UV-Vis) and Fourier transform infrared (FTIR) spectroscopy, combined with chemometric data fusion, was conducted to assess the metabolic profiles. Principal component analysis (PCA) and orthogonal partial least squares discriminant analysis (OPLS-DA) were performed to evaluate the data, facilitating robust classification and accurate identification of the key metabolites. Volcano plot analysis indicated that the soil-grown plants accumulated higher levels of phenolics and flavonoids, whereas hydroponic cultivation favored the synthesis of photosynthetic pigments and membrane lipids. The PCA revealed distinct separation between the groups, with PC1 explaining 84.8% and 69.2% of the FTIR and UV-Vis variance, respectively. OPLS-DA models exhibited the highest classification accuracy (100%) with  $R^2Y > 0.99$  and  $Q^2 > 0.98$ . Notably, low-level data fusion further enhanced discrimination, increasing predictive variance to 76.0% and capturing subtle metabolic differences that single techniques cannot detect. These results suggested that soil cultivation promotes a defensive metabolic strategy that enhances the antioxidant capacity, whereas hydroponic systems support growth-oriented metabolism. The integrative chemometric and data fusion approach provided a comprehensive metabolomic fingerprint, offering valuable insights into the optimization of cultivation practices to enhance the nutritional and functional values of *A. tricolor* L.

**Keywords:** *Amaranthus tricolor* L., Ultraviolet-Visible, Fourier Transform Infrared, Data Fusion, Chemometrics, Hydroponics, Soil-Grown

## Introduction

*Amaranthus tricolor* L., commonly recognized for its nutritional richness and bioactive compounds, has garnered increasing attention as a functional food.<sup>1</sup> It is known for its abundant vitamins, minerals,<sup>2,3</sup> and various bioactive elements,<sup>4-8</sup> including antioxidants,<sup>9,10</sup> antimicrobials,<sup>11</sup> neuroprotective,<sup>12</sup> hepatoprotective,<sup>13</sup> and anti-inflammatory agents,<sup>14</sup> all of which are associated with a range of health benefits. These bioactive compounds have spurred growing interest for their potential therapeutic applications in various diseases. Despite extensive studies on its nutrient profile, there is a significant gap in our understanding of the effects of environmental conditions, particularly the choice of growth media, on its metabolite composition. Previous research has explored how different cultivation systems, such as hydroponic and soil-based methods, affect the metabolite profiles of other plants, e.g., lettuce,<sup>15</sup> sweet potato,<sup>16</sup> *Rheum tibeticum*,<sup>17</sup> and *Helichrysum odoratissimum*.<sup>18</sup> However, the effects of these cultivation systems on the bioactive compound profiles of *A. tricolor* L. remain largely unknown.

\*Corresponding author. Email: [adlissantoni@sci.unand.ac.id](mailto:adlissantoni@sci.unand.ac.id)  
Tel: +62 821-7127-5982

**Citation:** Muthia A, Syukri D, Efdi M, Santoni A. Rapid Spectroscopy-based fingerprinting combined with data fusion chemometrics of *Amaranthus tricolor* L. for growing environment discrimination. Trop J Nat Prod Res. 2025; 9(10): 4933 – 4938 <https://doi.org/10.26538/tjnpr/v9i10.33>

Official Journal of Natural Product Research Group, Faculty of Pharmacy, University of Benin, Benin City, Nigeria

The adoption of hydroponic cultivation as an alternative to conventional soil-based farming presents a unique opportunity to investigate its effects on plant bioactive properties. Hydroponic systems offer precise control over environmental factors such as nutrient supply, pH, temperature, and light, which can enhance plant growth and elevate the levels of primary metabolites.<sup>19</sup> In contrast, soil-based cultivation is affected by the natural soil composition, water availability, and other external factors, which may trigger adaptive responses that influence the accumulation of specific metabolites, often acting as protective mechanisms against environmental stress or herbivory.<sup>20</sup> These contrasting cultivation systems likely result in substantial differences in the metabolite profiles of plants; however, the effects of these systems on *A. tricolor* L. have not been adequately investigated.

This study aimed to fill this knowledge gap by conducting a comparative analysis of the metabolite profiles of *A. tricolor* L. cultivated in hydroponic and soil-based systems. Through ultraviolet-visible (UV-Vis) and Fourier transform infrared (FTIR) spectroscopy, this study identified and compared the key bioactive compounds by categorizing samples based on their cultivation environment. UV-Vis spectroscopy is particularly effective for the quantitative analysis of specific metabolites, whereas FTIR spectroscopy provides insights into structural characteristics and allows functional group identification.<sup>21,22</sup> By integrating both techniques, this study enhances the comprehensiveness and reliability of metabolite profiling, offering a more holistic view of the influence of the cultivation environment on the bioactive properties of the plant. These findings provide a valuable reference for optimizing the cultivation practices of *A. tricolor* L., potentially enhancing its therapeutic potential and overall quality as a functional food.

## Materials and Methods

### Cultivation and preparation of samples

*A. tricolor* L. (Mira var., Panah Merah, Indonesia) was cultivated on a farm from July to August 2024 in Padang (0°56'57.26" N 100°21'15.37" E), Indonesia. In soil-based cultivation, plants were grown in 200 × 20 cm plots enriched with humus and manure, watered twice daily, and supplemented with a ZA/KCl/NPK fertilizer mix (1:1:1) in the first week after planting. In the hydroponic system, seedlings were initially placed on rockwool for five days before being transferred to a nutrient solution, AB mix (Infarm, Indonesia), with a total dissolved solid (TDS) concentration of 500–800 ppm (mg/L). All plants were harvested after a 24-day growth period. The specimen was deposited in the Herbarium of Universitas Andalas under voucher number ANDA00052507. The collected samples were lyophilized, homogenized in liquid nitrogen, and stored at −4 °C until further analysis.

### Spectral data acquisition

A homogeneous powder (10 mg) was dissolved in 10 mL of methanol (Merck, 99.9%, analysis grade, Germany) for UV-Vis spectroscopy. The solution was sonicated for 30 min and filtered. The spectra were recorded over a wavelength range of 200–800 nm every 0.5 nm, with methanol as the blank, using a UV-1800 series spectrophotometer (Shimadzu, Japan).<sup>21</sup> FTIR spectroscopy was conducted using the potassium bromide method with several modifications.<sup>23</sup> A 5 mg portion of the sample powder was mixed with potassium bromide (Sigma-Aldrich, USA) at a 1:3 (w/w) ratio, finely ground, and pressed into pellets for analysis. FTIR spectra were recorded using an IRTracer-100 spectrometer (Shimadzu, Japan) over the range of 4000–400 cm<sup>−1</sup>. All procedures were repeated five times to ensure reliability and reproducibility. The hydroponic samples were designated as HW, whereas the soil-grown samples were labeled as CW.

### Data pre-processing and statistical analysis

The collected spectral data were preprocessed and analyzed applying chemometric techniques with the R statistical software (version

2025.05.0) using the basic *prospectr* and *stats* packages. Following the modified Cavdaroglu and Ozen (2023) method,<sup>24</sup> the spectral data were preprocessed using the Savitzky–Golay smoothing method with a third-order polynomial and a window size of 31. Numerical variables were standardized using the standard normal-variate (SNV) technique. Volcano plots were used to evaluate the statistical significance using the t-test, followed by Log<sub>2</sub> Fold Change (log<sub>2</sub> FC). The results were considered statistically significant at a *p*-value < 0.05 and log<sub>2</sub> FC > 1. Principal component analysis (PCA) and orthogonal partial least squares discriminant analysis (OPLS-DA) were performed using the *ropls* package. Both low- and mid-level data fusion approaches were applied to examine whether the integration of datasets could improve model classification.<sup>25</sup>

## Results and Discussion

### Ultraviolet-visible and Fourier transform infrared spectra

UV-Vis and FTIR spectroscopic analyses were conducted to evaluate the metabolic profiles of *A. tricolor* L. grown in hydroponic (HW) and soil (CW) systems. The UV-Vis spectra (Figure 1a, Table 1) revealed several distinct absorption peaks indicative of various plant metabolites. In the UV region, absorption maxima were observed at 260, 267.5, and 318 nm, corresponding to the conjugated aromatic ring and heterocyclic chromophores that are characteristic of phenolics, flavonoids, and alkaloids, respectively.<sup>26,27</sup> Absorption bands in the visible region were identified at approximately 430 and 660 nm, corresponding to chlorophyll, and between 450 and 500 nm, indicating the presence of carotenoids.<sup>28</sup> The peak in the red-purple region at approximately 600–650 nm was attributed to anthocyanins, which was consistent with the known metabolite profile of the *Amaranthus* genus.<sup>26</sup> Notably, the HW samples exhibited higher absorption intensities at 409.5, 469, and 664.5 nm, suggesting elevated accumulation of chlorophyll and carotenoids.<sup>29</sup> Conversely, the CW samples exhibited higher absorption in the ultraviolet (200–350 nm) and visible (505.5–606 nm) ranges, indicating a higher concentration of phenolics, flavonoids, and anthocyanins.

**Table 1:** UV-Vis peak value and possible *A. tricolor* L. compound

Electronic transition	Peak value (nm)	Functional group	Representative compound	Volcano plot direction
UV region (200–350 nm)				
$\pi \rightarrow \pi^*$	260	Aromatic ring	Polyphenols, phenolics, flavonoids, alkaloids	HW (288 nm)
	267.5			CW (245 nm)
$n \rightarrow \pi^*$	318.5	Carbonyl		CW (367 nm)
Visible region (400–700 nm)				
$\pi \rightarrow \pi^*$ (extended)	409.5–535.5	Conjugated double bond	Chlorophylls and carotenoids	HW (415 nm)
	606–664.5		Anthocyanins	CW (428.5 nm)

**Note:** HW (hydroponic); CW (soil-grown)

The FTIR spectra provided additional insights into the molecular composition of *A. tricolor* L. grown under different conditions. Figure 2a and Table 2 present the FTIR absorption bands associated with the key functional groups, including the hydroxyl (O–H), carbonyl (C=O), aromatic (C=C), and ether (C–O–C) groups, which are characteristic of cellulose, hemicellulose, and lignin.<sup>30</sup> Although some bands overlapped with primary metabolites, distinct peaks were observed in specific regions, providing clear markers for secondary metabolites such as phenolics, flavonoids, and alkaloids. The peaks observed at 3399–3352

and 1639 cm<sup>−1</sup> correspond to O–H and aromatic C=C groups, signaling the presence of phenolic compounds.<sup>31</sup> Additionally, the absorption bands at 1736 cm<sup>−1</sup> (C=O stretch) and 1248 cm<sup>−1</sup> (C–O stretch) were indicative of esterified flavonoids or saponins.<sup>32</sup> Alkaloid-related N–H and C–N bands at approximately 1550 and 1320 cm<sup>−1</sup> further supported the presence of alkaloids, such as berberine-type compounds reported in the *Amaranthus* genus,<sup>33</sup> in the samples.

**Table 2:** FTIR peak values and functional groups of *A. tricolor* L.

Peak value (cm <sup>−1</sup> )	Vibrations	Functional group	Representative compound	Volcano plot direction
3399.59	O–H/N–H stretch	Hydroxyl/NH	Polysaccharides, protein, phenolics,	-
3352.34			flavonoids, alkaloids	
2927.99	C–H stretch	Alkyl	Lipids, lignin, terpenoids, steroids,	HW (2792.01 cm <sup>−1</sup> )
2857.59			alkaloids	
1735.96	C=O stretch	Carbonyl, ester	Hemicellulose, lignin, phenolics,	-
			flavonoids, terpenoids	
1639.82	C=C stretch	Aromatic, amide I	Proteins, phenolics, flavonoids, alkaloids	-
1546.93	N–H bend/C–N stretch	Amide II	Proteins, alkaloids	-
1376.23	C–H bend	Methyl	Polysaccharides, proteins, terpenoids,	-
			phenolics	

1327.05	O-H bend/C-N stretch		Polysaccharides, proteins, alkaloids, saponins	-
1247.96	C-O stretch	Ether, ester	Hemicellulose, flavonoid saponins	-
1157.31	C-O/C-O-C stretch	Alcohol, ether	Carbohydrates, flavonoid saponins, tannins	-
1107.16				
1070.51				
829.40	C=C out-of-plane bend	Aromatic rings	Phenolics, flavonoids,	CW (850.62 cm <sup>-1</sup> )
783.11				

**Note:** HW (hydroponic); CW (soil-grown)

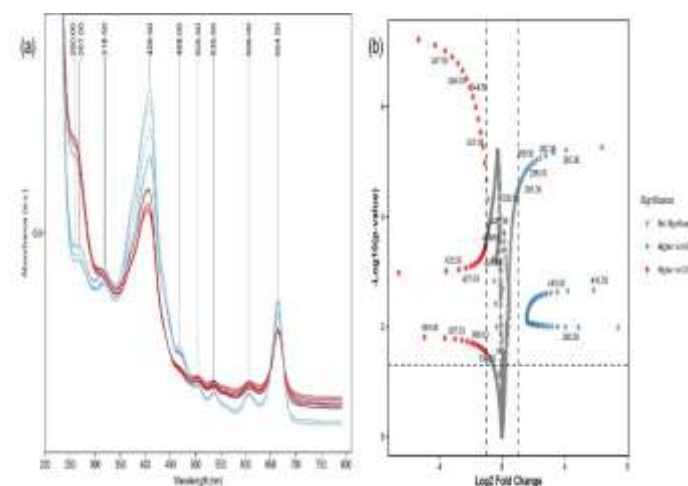


**Figure 1:** (a) Overlay visualization and (b) volcano plot of *A. tricolor* L. UV-Vis spectra

The FTIR results revealed that the HW samples accumulated phenolics, lignin, and nitrogen-containing compounds, with higher absorption of hydroxyls and amines at approximately 3300 and 1300 cm<sup>-1</sup>, respectively. By contrast, the CW samples exhibited stronger absorption in the fingerprint region (<1000 cm<sup>-1</sup>), indicating a higher concentration of complex metabolites. These results confirmed that hydroponically grown *A. tricolor* L. exhibited a higher accumulation of phenolic and nitrogen-containing compounds, whereas the soil-grown plants had elevated levels of complex compounds, including glycosylated phenolics and anthocyanins. These findings underscore the influence of the cultivation environment on metabolite accumulation, reflecting an adaptive response to environmental conditions.<sup>15</sup>

#### Chemometric analysis

Volcano plots were constructed using spectral data preprocessed by Savitzky–Golay smoothing and SNV normalization to statistically evaluate the chemical differences between the two cultivation systems. The volcano plot analysis, applying a significance threshold of  $-\log(p) > 1.5$  ( $p < 0.0316$ ) and  $|\log \text{ Fold Change}| > 1$ , highlighted three significant wavelengths in the UV-Vis spectra that distinguished the CW and HW samples (Figure 1b), which were located at 245 nm (aromatic rings), 367 nm (flavonol B-ring excitations), and 428.5 nm (carotenoids and anthocyanins). The higher absorption at these wavelengths in the CW samples reflected the elevated accumulation of defensive phenolic compounds and pigment precursors, likely induced by abiotic stress that activates phenylpropanoid biosynthesis.<sup>34</sup> In contrast, the HW samples exhibited enhanced absorption at 288 nm (phenolic acid carbonyl) and 415 nm (chlorophyll-related porphyrin), suggesting an increase in photosynthetic pigments and simpler phenolic compounds, which aid in light-capturing efficiency.<sup>29</sup> The FTIR volcano plot (Figure 2b) further corroborates these observations. The peaks for the CW samples exhibited higher intensities at 850.62 cm<sup>-1</sup> (C–H bending of aromatics) and 2832.51 cm<sup>-1</sup> (C–H stretching of fatty acid chains), which are the markers of phenolic polymers and lipid-derived components. These results are consistent

with the UV-Vis results depicting the elevated levels of secondary metabolites in soil-grown *A. tricolor* L. The HW samples exhibited higher absorption at 2792.97 cm<sup>-1</sup> (C–H stretching of aromatic aldehydes), suggesting an enhancement of phenolic aldehydes, likely due to altered carbon fluxes under hydroponic conditions.<sup>35</sup> These spectral analyses indicate that hydroponic cultivation leads to increased synthesis of photosynthetic pigments and membrane lipids, along with an altered profile of secondary metabolites, which may favor precursor amino acids and intermediate phenolic aldehydes.<sup>29</sup> Soil-based systems promote the production of metabolites, such as phenolics and flavonoids, which strengthen plant defense mechanisms.<sup>36</sup>

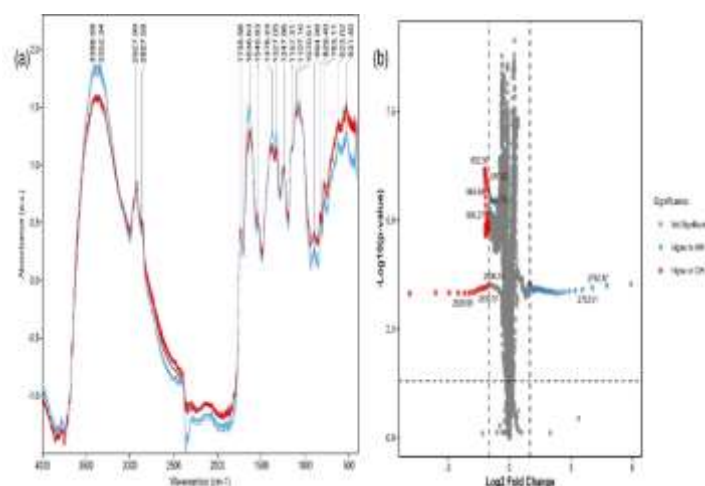


**Figure 2:** (a) Overlay visualization and (b) volcano plot of *A. tricolor* L. FTIR spectra

PCA and OPLS-DA were performed to explore multivariate differences in the chemical composition of the samples. The PCA score plots (Figure 3) separated the HW and CW samples along principal components 1 (PC1) and 2 (PC2), which explained the major variance in the data. For the FTIR spectra, PC1 accounted for 84.8% of the variance, whereas for the UV-Vis spectra, it accounted for 69.2%. This demonstrates that both techniques can differentiate the two cultivation methods. The application of data fusion at a low-level integration further improved the separation, retaining the full spectral resolution of both FTIR and UV-Vis data while enhancing the classification power. In this case, PC1 explained 78.6% of the variance, approaching the discriminatory capacity of the FTIR data alone, while incorporating complementary pigments and phenolic features from the UV-Vis spectra. Mid-level fusion, which combines higher-order components, resulted in a lower PC1 contribution (49.9%), suggesting that this approach captured more balanced and subtle interactions between the techniques.<sup>37</sup> OPLS-DA further refined the separation of the samples by emphasizing the components that maximized group separation and orthogonalized unrelated spectral variations. The OPLS-DA score plots revealed sharper distinctions between the HW and CW samples, particularly in FTIR and low-level fusion analyses. The performance of the OPLS-DA (Table 3) models was assessed using the goodness of fit (R<sup>2</sup>Y) and goodness of prediction (Q<sup>2</sup>). Both metrics exceeded 0.90, indicating excellent model performance.<sup>38</sup>

matrix); Q<sup>2</sup> by CV (prediction ability of the model by cross-validation); RMSEE (root mean square error of estimation).

The root mean squared error of the estimation (RMSEE) ranged from 0.038 to 0.044, demonstrating minimal prediction errors.<sup>39</sup> Notably, the predictive variance (t<sub>1</sub>P) was the highest for the FTIR (0.828) and low-level fusion (0.760) datasets, highlighting the superior discriminatory ability of these strategies. The OPLS-DA models achieved near-perfect classification metrics with 100% accuracy, sensitivity, and specificity.<sup>24</sup> Cross-validation and permutation testing further validated the models with *p*-value < 0.05, confirming their robustness and minimizing the risk of overfitting.

Our results align with the findings of previous studies on the effects of cultivation methods on plant secondary metabolites. In a study analyzing polyphenols in mature seeds of 18 *Amaranthus* genotypes, PCA showed that environmental conditions had a significant effect on the levels of flavonoids such as rutin and nicotiflorin.<sup>40</sup> Nekesa et al. (2025) showed that hydroponically grown tomatoes and spinach possessed higher levels of α-tocopherol and β-carotene.<sup>41</sup> Another study reported a higher accumulation of lignin in hydroponic lettuce (22.5%) than in that grown in soil.<sup>34</sup> However, soil-grown plants had elevated levels of phenolics, flavonoids, and anthocyanins, especially trans-*p*-coumarin, isorhamnetin-3-*O*-glucoside, and nicotiflorin from wild *Amaranthus viridis*.<sup>42</sup> A previous study on herbal aromatics and lettuce consistently revealed higher total phenolic and flavonoid contents in soil-grown plants than in hydroponically grown plants.<sup>43</sup> This finding confirms that hydroponic systems enhance growth-related metabolites, whereas soil systems promote defense-related compounds. Additionally, the integration of UV-Vis and FTIR spectroscopy in our study allowed the comprehensive analysis of both primary and secondary metabolites, similar to the combination of these techniques in other studies to explore plant metabolic profiles.<sup>44–46</sup> Previous studies have shown that data fusion strategies are superior in authenticating *Dendrobium* species although they are dominated by data with more variables (FTIR data).<sup>47</sup> However, the integration of UV-Vis and FTIR data does not always result in a significant increase in efficiency. This is because information from a single spectral dataset is sufficient for classification, as reported in the quality analysis of mint.<sup>48</sup> Data fusion methods improve the resolution of spectral analyses and enhance the differentiation between plant samples grown under different conditions.

Conclusion

This study highlighted the significant effect of cultivation methods on the metabolite profile of *A. tricolor* L. Notably, hydroponic cultivation was linked to a higher accumulation of photosynthetic pigments and membrane lipids, whereas soil-based cultivation favored the production of secondary metabolites, including phenolics and flavonoids, which are critical for plant defense. The integration of UV-Vis and FTIR spectroscopy through chemometric data fusion enhanced the discrimination between the samples from these two cultivation systems. Multivariate analyses, such as PCA and OPLS-DA, revealed substantial metabolite variations that might have been overlooked by traditional methods, with FTIR alone explaining 82.8% of the variance. The high predictive performance of the models, evidenced by R<sup>2</sup>Y and Q<sup>2</sup> values exceeding 0.99 and 0.98, respectively, confirms the robustness and utility of these techniques for assessing metabolite profiles. These results suggest that cultivation systems can be strategically selected to optimize bioactive compound accumulation based on specific functional properties. Future research should focus on expanding the environmental conditions under which *A. tricolor* L. is cultivated using controlled settings to validate these findings. Additionally, the exploration of long-term cultivation effects and other potential factors, such as light intensity and nutrient availability, would provide valuable insights into the optimization of plant metabolite profiles for therapeutic applications.

Conflict of Interest

The author's declare no conflict of interest.

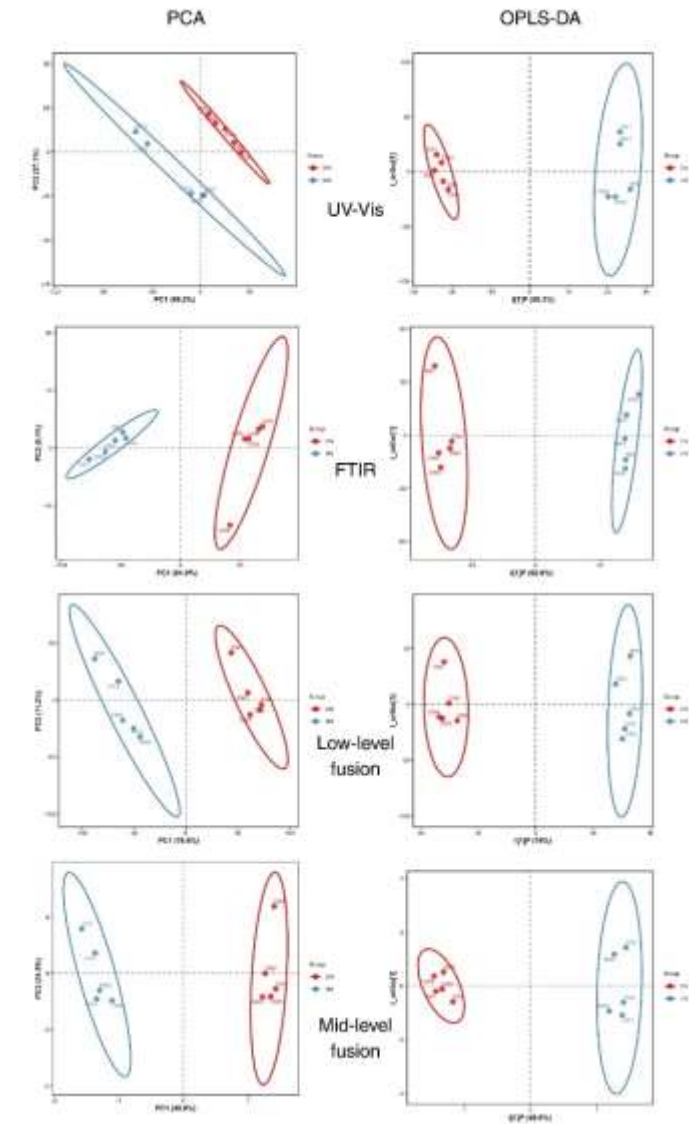


**Figure 3:** Principal component analysis (PCA) and orthogonal partial least squares discriminant analysis (OPLS-DA) for FTIR, UV-Vis, low-level, and mid-level data fusion spectra of *A. tricolor* L.

Table 3: Summary of the OPLS-DA validation model performance				
OPLS-DA Metric Performances	FTIR	UV-Vis	Low-Level	Mid-Level
R <sup>2</sup> Y	0.996	0.995	0.996	0.995
Q <sup>2</sup> (by CV)	0.988	0.993	0.987	0.989
RMSEE	0.038	0.042	0.039	0.044
Predictive Variance (t <sub>1</sub> P)	0.828	0.503	0.760	0.498
Accuracy (Training)	1	1	1	1
Sensitivity (HW)	1	1	1	1
Specificity (CW)	1	1	1	1
<i>p</i> -value (R <sup>2</sup> Y)	0.010	0.020	0.015	0.020
<i>p</i> -value (Q <sup>2</sup> )	0.010	0.020	0.015	0.020

**Note:** OPLS-DA (orthogonal partial least squares discriminant analysis); FTIR (Fourier transform infrared spectroscopy); UV-Vis (ultraviolet-visible); R<sup>2</sup>Y (measured rate of the built model for the Y



## Authors' Declaration

The authors hereby declare that the work presented in this article is original and that any liability for claims relating to the content of this article will be borne by them.

## Acknowledgements

The authors would like to express their sincere gratitude to LPPM Universitas Andalas for the financial support provided through the Penelitian Disertasi Doktor (PDD) Scheme Batch I under Decree Nos. 12/KPT/R/PTN-BH/UNAND/2024 and Agreement/Contract Nos. 21/UN16.19/PT.01.03/PDD/2024.

## References

- Sarker U, Oba S, Ullah R, Bari A, Ercisli S, Skrovankova S, Adamkova A, Zvonkova M, Mlcek J. Nutritional and bioactive properties and antioxidant potential of *Amaranthus tricolor*, *A. lividus*, *A. viridis*, and *A. spinosus* leafy vegetables. *Heliyon*. 2024; 10(9): e30453. Doi: 10.1016/j.heliyon.2024.e30453.
- Shukla S, Bhargava A, Chatterjee A, Srivastava J, Singh N, Singh SP. Mineral profile and variability in vegetable amaranth (*Amaranthus tricolor*). *Plant Foods Hum Nutr*. 2006; 61(1): 23-28. Doi: 10.1007/3-7643-7438-1\_3.
- Sarker U, Islam MdT, Oba S. Salinity stress accelerates nutrients, dietary fiber, minerals, phytochemicals and antioxidant activity in *Amaranthus tricolor* leaves. *PLoS One*. 2018; 13(11): e0206388. Doi: 10.1371/journal.pone.0206388.
- Sumarmi S, Arlinda M, Sukirno S. The Effectiveness of Red Spinach (*Amaranthus tricolor* L.) and Green Spinach (*Amaranthus hybridus* L.) Extracts for *Bacillus thuringiensis* var. kurstaki Protectant against UVB Radiation for the Control of Armyworm (*Spodoptera litura* Fab.). *J Trop Biodivers Biotechnol*. 2020; 5(2): 143-148. Doi: 10.22146/jtbb.53004.
- Jang S, Shim J, Choe Y, Kim SJ, Kim TW. Biochemical analysis of Betalain Biosynthesis and Photosynthesis of Amaranth (*Amaranthus tricolor* L.) by Dessication under high-temperature. In: The 8th World Congress on New Technologies. Prague, 2022 doi:10.11159/icepr22.139.
- Jeong WT, Bang J-H, Han S, Hyun TK, Cho H, Lim H Bin, Chung J-W. Establishment of a UPLC-PDA/ESI-Q-TOF/MS-Based Approach for the Simultaneous Analysis of Multiple Phenolic Compounds in Amaranth (*A. cruentus* and *A. tricolor*). *Molecules*. 2020; 25(23): 5674. Doi: 10.3390/molecules25235674.
- Fei P, Feng H, Wang Y, Kang H, Xing M, Chang Y, Guo L, Chen J. *Amaranthus tricolor* crude extract inhibits *Cronobacter sakazakii* isolated from powdered infant formula. *J Dairy Sci*. 2020; 103(11): 9969-9979. Doi: 10.3168/jds.2020-18480.
- House NC, Puthenparampil D, Malayil D, Narayanankutty A. Variation in the polyphenol composition, antioxidant, and anticancer activity among different *Amaranthus* species. *S Afr J Bot*. 2020; 135: 408-412. Doi: 10.1016/j.sajb.2020.09.026.
- Gins MS, Gins VK, Motyleva SM, Kulikov IM, Medvedev SM, Pivovarov VF, Mertvishcheva ME. Metabolites with Antioxidant and Protective Functions from Leaves of Vegetable Amaranth (*Amaranthus tricolor* L.). *Agric Biol*. 2017; 52(5): 1030-1040. Doi: 10.15389/agrobiology.2017.5.1030eng.
- Spórna-Kucab A, Tekieli A, Grzegorzczak A, Skalicka-Woźniak K, Starzak K, Wybraniec S. Antioxidant and Antimicrobial Effects of Baby Leaves of *Amaranthus tricolor* L. Harvested as Vegetable in Correlation with Their Phytochemical Composition. *Molecules*. 2023; 28(3): 1463. Doi: 10.3390/molecules28031463.
- Li-wei G, Wang Y, Bi X, Duo K, Sun Q, Yun X, Zhang H, Peng F, Han J. Antimicrobial Activity and Mechanism of Action of the *Amaranthus Tricolor* Crude Extract Against *Staphylococcus Aureus* and Potential Application in Cooked Meat. *Foods*. 2020; 9(3): 359. Doi: 10.3390/foods9030359.
- Bala VC, Abid M. Neuroprotective Effect of Hydroalcoholic Extract of *Amaranthus tricolor* Leaves On Experimental. *Asian J Pharm Clin Res*. 2020; 13: 181-186. Doi: 10.22159/ajpcr.2020.v13i6.37181.
- Ehi-Omosun MB, Omoko OG. Effects of Aqueous Leaf Extract of *Amaranthus tricolor* On the Liver of the Adult Wistar Rat. *Journal of Applied Sciences and Environmental Management*. 2023; 27(4): 879-882. Doi: 10.4314/jasem.v27i4.33.
- Bihani GV, Bodhankar SL, Kadam PP, Zambare GN. Antinociceptive and anti-inflammatory activity of hydroalcoholic extract of leaves of *Amaranthus tricolor* L. *Pharm Lett*. 2013; 5(3): 48-55.
- Hameed MK, Umar W, Razzaq A, Aziz T, Maqsood MA, Wei S, Niu Q, Huang D, Chang L. Differential Metabolic Responses of Lettuce Grown in Soil, Substrate and Hydroponic Cultivation Systems under  $\text{NH}_4^+/\text{NO}_3^-$  Application. *Metabolites*. 2022; 12(5): 444. Doi: 10.3390/metabo12050444/S1.
- Lin Z, Li G, Zhang H, Ji R, Xu Y, Xu G, Li H, Liu Z, Luo W, Qiu Y, Qiu S, Tang H. Metabolic characteristics of taste differences under the soil and hydroponic cultures of sweet potato leaves by using non-targeted metabolomics. *bioRxiv*. 2021; 93(12). Doi: 10.1101/2021.02.24.432602.
- Giri L, Angmo JC, Hussain M, Singh B, Bhatt ID, Nautiyal S. Hydroponic culture improves growth and secondary metabolite production in *Rheum tibeticum*, a near threatened species from the Ladakh Trans-Himalayan region of India. *Plant Biosystems*. 2025; 159(2): 356-368. Doi: 10.1080/11263504.2025.2468727.
- Zantanta N, Kambizi L, Etsassala NGER, Nchu F. Comparing Crop Yield, Secondary Metabolite Contents, and Antifungal Activity of Extracts of *Helichrysum odoratissimum* Cultivated in Aquaponic, Hydroponic, and Field Systems. *Plants*. 2022; 11(20): 2696. Doi: 10.3390/plants11202696.
- Buitrago-Villanueva I, Barbosa-Cornelio R, Coy-Barrera E. Specialized Metabolite Profiling-Based Variations of Watercress Leaves (*Nasturtium officinale* R.Br.) from Hydroponic and Aquaponic Systems. *Molecules*. 2025; 30(2): 406. Doi: 10.3390/molecules30020406.
- Hu L, Wu Z, Robert CAM, Ouyang X, Züst T, Mestrot A, Xu J, Erb M. Soil chemistry determines whether defensive plant secondary metabolites promote or suppress herbivore growth. In: *Proceeding of the National Academy of Sciences of the United States of America*. 2021, p e2109602118.
- Arifah MF, Hastuti AA, Rohman A. Utilization of UV-visible and FTIR spectroscopy coupled with chemometrics for differentiation of Indonesian tea: an exploratory study. *Indones J Pharm*. 2022; 33: 200-207. Doi: 10.22146/ijp.3795.
- Sharma A, Mazumdar B, Keshav A. Extraction and Phytochemical Analysis of *Coccinia indica* Fruit Using UV-VIS and FTIR Spectroscopy. In: *International Conference on Biomedical Engineering Science and Technology: Roadway from Laboratory to Market*. Springer Nature: Chhattisgarh, India, 2021, pp 1-7.
- Rafi M, Rismayani W, Sugiarti RM, Syafitri UD, Wahyuni WT, Rohaeti E. FTIR-based fingerprinting combined with chemometrics for discrimination of *Sonchus arvensis* leaves extracts of various extracting solvents and the correlation with its antioxidant activity. *Indones J Pharm*. 2021; 32: 132-140. Doi: 10.22146/ijp.755.
- Cavdaroglu C, Ozen B. Applications of UV-Visible, Fluorescence and Mid-Infrared Spectroscopic Methods Combined with Chemometrics for the Authentication of Apple Vinegar. *Foods*. 2023; 12(6): 1139. Doi: 10.3390/foods12061139.
- Azcarate SM, Ríos-Reina R, Amigo JM, Goicoechea HC. Data handling in data fusion: Methodologies and applications. *TrAC*. 2021; 143: 116355. Doi: 10.1016/j.trac.2021.116355.
- Sarker U, Oba S. Polyphenol and flavonoid profiles and radical scavenging activity in leafy vegetable *Amaranthus gangeticus*. *BMC Plant Biol*. 2020; 20(1): 499. Doi: 10.1186/s12870-020-02700-0.
- Mabasa XE, Mathomu LM, Madala NE, Musie EM, Sigidi MT. Molecular Spectroscopic (FTIR and UV-Vis) and Hyphenated Chromatographic (UHPLC-qTOF-MS) Analysis and In Vitro

- Bioactivities of the *Momordica balsamina* Leaf Extract. *Biochem Res Int.* 2021; 2021(1): 1-12. Doi: 10.1155/2021/2854217.
- 28 Nyonje WA, Schafleitner R, Abukutsa-Onyango M, Yang RY, Makokha A, Owino W. Precision phenotyping and association reveal increased water use efficiency and higher lycopene and  $\beta$ -carotene contents in hydroponically grown tomatoes. *Sci Hortic.* 2021; 279: 109896. Doi: 10.1016/j.scienta.2021.109896.
  - 30 He Z, Liu Y, Kim HJ, Tewolde H, Zhang H. Fourier transform infrared spectral features of plant biomass components during cotton organ development and their biological implications. *J. Cotton Sci.* 2022; 5(1): 11. Doi: 10.1186/s42397-022-00117-8.
  - 31 Chaturvedi S, Gupta P. Evaluation of Bioactive Metabolites and Antioxidant-Rich Extracts of Amaranths with Possible Role in Pancreatic Lipase Interaction: In Silico and In Vitro Studies. *Metabolites.* 2021; 11(10): 676. Doi: 10.3390/metabo11100676.
  - 32 Schröter D, Baldermann S, Schreiner M, Witzel K, Maul R, Rohn S, Neugart S. Natural diversity of hydroxycinnamic acid derivatives, flavonoid glycosides, carotenoids and chlorophylls in leaves of six different amaranth species. *Food Chem.* 2018; 267: 376-386. Doi: 10.1016/j.foodchem.2017.11.043.
  - 33 Al-Tamimi A, Alfarhan A, Al-Ansari A, Rajagopal R. Antioxidant, enzyme inhibitory and apoptotic activities of alkaloid and flavonoid fractions of *Amaranthus spinosus*. *Physiol Mol Plant Pathol.* 2021; 116: 101728. Doi: 10.1016/j.pmpp.2021.101728.
  - 34 Lei C, Engeseth NJ. Comparison of growth characteristics, functional qualities, and texture of hydroponically grown and soil-grown lettuce. *LWT.* 2021; 150: 111931. Doi: 10.1016/j.lwt.2021.111931.
  - 35 Lin Z, Li G, Zhang H, Ji R, Xu Y, Xu G, Li H, Liu Z, Luo W, Qiu Y, Tang H, Qiu S. Metabolic Characteristics of Taste Differences of Sweet Potato Leaves Grown in Soil and Hydroponic Cultures by Using Non-Targeted Metabolomics. *Phyton (B Aires).* 2024; 93(12): 3401-3410. Doi: 10.32604/phyton.2024.058692.
  - 36 Gfeller V, Waelchli J, Pfister S, Deslandes-Hérolde G, Mascher F, Glauser G, Aeby Y, Mestrot A, Robert CAM, Schlaeppli K, Erb M. Plant secondary metabolite-dependent plant-soil feedbacks can improve crop yield in the field. *Elife.* 2023; 12: e84988. Doi: 10.7554/eLife.84988.
  - 37 Leng H, Chen C, Chen C, Chen F, Du Z, Chen J, Yang B, Zuo E, Xiao M, Lv X, Liu P. Raman spectroscopy and FTIR spectroscopy fusion technology combined with deep learning: A novel cancer prediction method. *Spectrochim Acta A Mol Biomol Spectrosc.* 2023; 285: 121839. Doi: 10.1016/j.saa.2022.121839.
  - 38 Ren X, Li S, Zhang M, Guan L, Han W. Geographical discrimination of fresh instant rice according to non-destructive analysis of flavor profiles. *Cereal Chem.* 2023; 100(2): 414-423. Doi: 10.1002/cche.10621.
  - 39 Ikram MMM, Ridwani S, Putri SP, Fukusaki E. GC-MS Based Metabolite Profiling to Monitor Ripening-Specific Metabolites between morphological traits and nutritional content in Vegetable Amaranth (*Amaranthus spp.*). *J Agric Food Res.* 2021; 5: 100165. Doi: 10.1016/J.JAFR.2021.100165.
  - 29 Verdoliva SG, Gwyn-Jones D, Detheridge A, Robson P. Controlled comparisons between soil and hydroponic systems in Pineapple (*Ananas comosus*). *Metabolites.* 2020; 10(4): 134. Doi: 10.3390/metabo10040134.
  - 40 Schröter D, Baldermann S, Schreiner M, Witzel K, Maul R, Rohn S, Neugart S. Natural diversity of hydroxycinnamic acid derivatives, flavonoid glycosides, carotenoids and chlorophylls in leaves of six different amaranth species. *Food Chem.* 2018; 267: 376-386. Doi: 10.1016/j.foodchem.2017.11.043.
  - 41 Nekesa R, Njue LG, Abong GO. A Comparative Analysis on the Variation of  $\beta$ -Carotene, Vitamin C and E Levels in Hydroponic and Soil-Based Fruits and Vegetables in Kiambu County, Kenya. *Food Sci Nutr.* 2025; 13(6). Doi: 10.1002/fsn3.70403. doi:10.1002/fsn3.70403.
  - 42 Cunha-Chiamolera TPL da, Chieleh-Chelh T, Urrestarazu M, Ezzaitouni M, López-Ruiz R, Gallón-Bedoya M, Rincón-Cervera MÁ, Guil-Guerrero JL. Crop Productivity, Phytochemicals, and Bioactivities of Wild and Grown in Controlled Environment Slender Amaranth (*Amaranthus viridis* L.). *Agronomy.* 2024; 14(9): 2038. Doi: 10.3390/agronomy14092038.
  - 43 Mampholo BM, Truter M, Maboko MM. Yield, Phytonutritional and Essential Mineral Element Profiles of Selected Aromatic Herbs: A Comparative Study of Hydroponics, Soilless and In-Soil Production Systems. *Plants.* 2025; 14(14): 2179. Doi: 10.3390/plants14142179.
  - 44 Yao S, Li T, Liu H, Li J, Wang Y. Traceability of *Boletaceae* mushrooms using data fusion of UV-visible and FTIR combined with chemometrics methods. *J Sci Food Agric.* 2018; 98(6): 2215-2222. Doi: 10.1002/jsfa.8707.
  - 45 Yao S, Li T, Li J, Liu H, Wang Y. Geographic identification of Boletus mushrooms by data fusion of FT-IR and UV spectroscopies combined with multivariate statistical analysis. *Spectrochim Acta A Mol Biomol Spectrosc.* 2018; 198: 257-263. Doi: 10.1016/j.saa.2018.03.018.
  - 46 Zhi W-X, Wang B-R, Zhou J, Qiu Y-C, Lu S-Y, Yu J-Z, Zhang Y-H, Mu Z-S. Rapid and accurate quantification of trypsin activity using integrated infrared and ultraviolet spectroscopy with data fusion techniques. *Int J Biol Macromol.* 2024; 278: 135017. Doi: 10.1016/j.ijbiomac.2024.135017.
  - 47 Wang Y, Zuo Z-T, Shen T, Huang H-Y, Wang Y-Z. Authentication of Dendrobium Species Using Near-Infrared and Ultraviolet-Visible Spectroscopy with Chemometrics and Data Fusion. *Anal Lett.* 2018; 51(17): 2792-2821. Doi: 10.1080/00032719.2018.1451874.
  - 48 Kucharska-Ambrożej K, Martyna A, Karpińska J, Kiełtyka-Dadasiewicz A, Kubat-Sikorska A. Quality control of mint species based on UV-VIS and FTIR spectral data supported by chemometric tools. *Food Control.* 2021; 129: 108228. Doi: 10.1016/j.foodcont.2021.108228.